2024 Tenth Indian Control Conference (ICC)
9 - 11 December, 2024
IISER Bhopal, India

Unified Dual-Wheel PID Control for Differential Drive Robot with Distinct Wheel Error Functions

Yogi Naragani[1], Deepak Singh Gariya[2] and Rahul Singhal[3]

Abstract— **The PID controller is the most versatile controller due to its ease of implementation. However, multi-input control design with PID controller is a challenging task. This paper presents the unified PID implementation for the right and left wheels of the differential drive robot. The distinct error function was considered for each wheel utilizing the robot's kinematic relationship. The simulation result of the proposed unified dual wheel PID (UDW-PID) controller presented for the straight, circular and sine path. The control action generated for the respective wheel resulted in smoother and quicker convergence towards the path, and afterwards stable behaviour over the path.**

I. INTRODUCTION

Nowadays, increasing production efficiency and meeting client demands in any industry necessitates process automation. Static machinery cannot complete this automation on its own without assistance. To fix this, machines must be able to move between sites and perform certain activities, such as material handling and autonomous vehicles without human supervision. Robotics is the study of creating intelligent devices [1] capable of performing a variety of tasks, such as moving across a space to move from one location to another [2]. Numerous industries, including manufacturing [3], healthcare [4], food processing, space exploration [5], and household appliances [6] have begun employing intelligent robots for accomplishing various tasks. In these industries, robots are utilized to reduce idle time and increase productivity. Robots are also used for duties that are hazardous to humans [7].

Proportional Integral Derivative (PID) controllers are widely utilized in industries for process automation [8]. Because PID controllers are not model-based, they can be easily implemented in a variety of systems. Compared to other control strategies, the PID controller is less expensive to implement. When tuned properly, the PID controller speeds up the system's approach to steady state. By minimizing steady state error, PID controllers remove oscillatory behavior in steady state [9]. The PID controller utilises the information of error from the desired reference which makes it a closed loop control strategy.

Despite the fact that the PID controller are non-model based controller.Designing a PID controller for a system might be challenging. The controller is highly sensitive to parameter changes. The gain parameters of the controller needs to be fine-tuned, which can be challenging task [8]. It can amplify noise, which adds to the unsteady behavior of the system. However, for systems with a single input and single output (SISO), the PID controllers are particularly advantageous. It might be challenging to implement a PID controller with multiple control inputs (MIMO) systems [10], which can cause instability in the control behavior. Differential drive robot has two control inputs namely ω_L and ω_R, hence a conventional PID controller is unsuitable for controlling it. Also, the conventional PID controller does not account for all the kinematic parameters of the robot [11]. It's possible that the conventional PID controller's single error function isn't the best way for controlling the differential drive robot, which may be suitable for few waypoints tracking. To control the differential drive robot high level control strategies such as MPC, LQR are usually used [12].

In this paper the proposed method is using a single PID controller with two distinct error functions for the left and right wheels of differential drive robot. The error function is based on the forward and inverse kinematics of the differential drive robot. The controller has only one set of gains K_p, K_i and K_d which are tuned for straight, circular and sinusoidal trajectories. This error function accounts for the all kinematic parameters of the robot. The error function takes errors in robot frame ($\mathbb{RF}$) corrects it in wheel frame ($\mathbb{WF}$) using PID controller. The control output is generated for the the left and right wheel of the robot with same PID gains but distinct error function for the each wheel.

The structure of the paper is as follows. To preserve the flow of the paper, differential drive robot kinematics and inverse kinematics models are presented in section 2. The new scheme proposed for the PID controller for the robot's left and right wheels is presented in section 3. The trajectory tracking considerations and simulation results with discussion are presented in section 4. After that, conclusions are drawn in section 5.

II. DIFFERENTIAL DRIVE ROBOT

In process automation, mobile robots are used for moving materials around the shop floor [13]. Among the robots Differential drive robots are the most often utilized mobile robots. These are simple to control [14] with inverse kinematics or any control strategy. Differential drive has a simpler structure compared to any other other mobile robot. It has two wheels that are attached to a motor to propel the robot. The two wheels are aligned on the common axis passing through the center of the wheel. A caster wheel is

[1]Yogi Naragani, [2]Deepak Singh Gariya, and [3]Rahul Singhal is with Department of Electrical Engineering, School of Advanced Engineering, UPES, Dehradun, India yogi.119192@stu.upes.ac.in, deepak.126198@stu.upes.ac.in, rahul.singhal@ddn.upes.ac.in

mounted on either the front or back end of the robot. To drive the robot, we must provide input voltage to two motors [15]. When the motors get the same input voltage, the robot moves in a straight line. To turn the robot inputting different voltages to the motors causes the robot to turn either right or left. The parameters of the differential drive [16] are shown in Fig:1 where L - distance between the surface contact points of two wheels, R - radius of each wheel. The turning radius is dependent on the distance between two wheels (L) and the wheel radius (R) which are constant for a robot once designed, whereas distance travelled is dependent on the wheel radius (R) only. Differential drive robots offer great maneuverability [17].

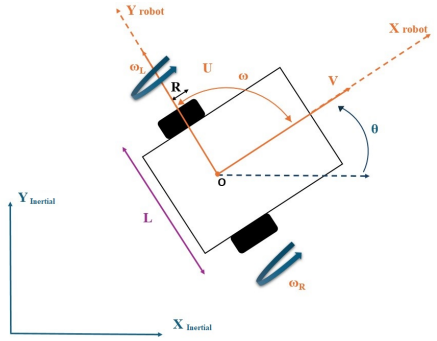


Fig. 1: Frames and Motion Representation of a Differential Drive Robot

A. Forward and Inverse Kinematics of Differential Drive Robot

The way point tracking of differential drive robot is done in three frames as shown in Fig:1. The first frame is the inertial frame represented as $\mathbb{IF}$. The $\mathbb{IF}$ is the reference frame for the robot. The position of the robot is described with respect to the $\mathbb{IF}$. Where, X - position of robot in $\mathbb{IF}$ along $X_{inertial}$, Y - position of robot along $Y_{inertial}$, and θ - orientation of the robot. The second frame is the $\mathbb{RF}$. In this frame the robot instantaneous velocities of the robot are described. Where, V - translational velocity in the robot, and ω -angular velocity of the robot. The third frame is wheel frame $\mathbb{WF}$, in this frame the two wheels rotational speeds are described [18]. Where, ω_L - angular velocity of the left wheel, and ω_R - angular velocity of the right wheel.

The forward kinematics of differential drive relates the rotational speeds of the two wheels in $\mathbb{WF}$ to its velocities in $\mathbb{RF}$ shown in (2). These velocities in $\mathbb{RF}$ are used to obtain the position of the robot in the $\mathbb{IF}$. Inverse kinematics [18] of differential drive involves for the desired new position in the $\mathbb{IF}$ obtaining the wheel rotational velocities in $\mathbb{WF}$.

$$\begin{bmatrix} V \\ w \end{bmatrix} = \begin{bmatrix} R/2 & R/2 \\ R/L & -R/L \end{bmatrix} \begin{bmatrix} \omega_L \\ \omega_R \end{bmatrix} \tag{1}$$

$$\underbrace{V, \omega}_{\mathbb{RF}} = f_{fk}(\underbrace{\omega_L, \omega_R}_{\mathbb{WF}}) \tag{2}$$

Forward kinematics function of the differential drive robot f_{fk} takes wheel angular velocities ω_L and ω_R in $\mathbb{WF}$ as inputs, and linear velocity V and angular velocity w as outputs in $\mathbb{RF}$.

$$\underbrace{\begin{bmatrix} X(i+1) \\ Y(i+1) \\ \theta(i+1) \end{bmatrix}}_{P(i+1)} = \underbrace{\begin{bmatrix} X(i) \\ Y(i) \\ \theta(i) \end{bmatrix}}_{P(i)} + \underbrace{\begin{bmatrix} V\ .\ cos(\theta(i)) \\ V\ .\ sin(\theta(i)) \\ \omega(i) \end{bmatrix}}_{velocity} .\ \triangle t \tag{3}$$

To calculate the new position of robot in $\mathbb{IF}$. V and ω are in $\mathbb{RF}$ and current position $P(i)$ of the robot at time instant i are considered [19].

$$\begin{bmatrix} \omega_L \\ \omega_R \end{bmatrix} = \begin{bmatrix} 1/R & -L/2 \\ 1/R & -L/2 \end{bmatrix} \begin{bmatrix} V \\ \omega \end{bmatrix} \tag{4}$$

$$\underbrace{\omega_L, \omega_R}_{\mathbb{WF}} = f_{ik}(\underbrace{V, \omega}_{\mathbb{RF}}) \tag{5}$$

Inverse Kinematics function of the differential drive f_{ik} robot takes translation velocity V and angular velocity ω in $\mathbb{RF}$ and outputs wheel angular velocities ω_L and ω_R in $\mathbb{WF}$ [20].

III. Unified Dual-Wheel PID Control

In traditional PID control error would be dependent on the single variable. Tuning gains for this for this single error is easier. The gains K_p, K_i and K_d are tuned to achieve the desired result. The gain K_p corresponds to the proportional of the error its effect diminishes as the error is being reduced. The gain K_i corresponds to the integral or sum of the previous errors. This gain plays a significant role in the steady state of the system. The last gain K_d is corresponds to the rate of change of error. In general PID implementation for differential drive robot, speed V is kept constant, error is taken as function of θ in $\mathbb{IF}$ which varies the ω in $\mathbb{RF}$. This doesn't always guarantee that robot follows the path precisely, and only well suited for tracking few way points on the path.

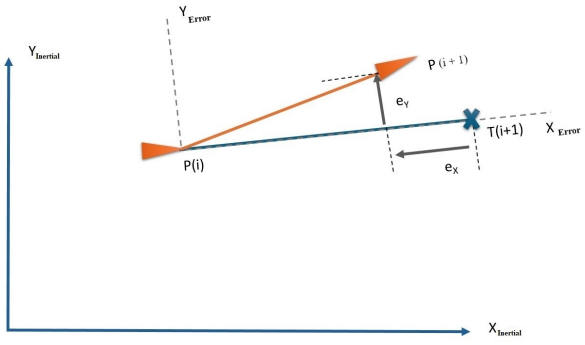


Fig. 2: Error components e_x and e_y in error frame $\mathbb{EF}$

In this proposed new PID control two error functions e_{ω_L} and e_{ω_R} are developed for left and right wheels of the differential drive robot shown in (14,15). The output of

the PID would be control input of ω_L and ω_R. The error functions are developed in the error frame $\mathbb{EF}$ to compensate for variables in $\mathbb{WF}$ shown in Fig:2. The origin of the $\mathbb{EF}$ lies on the current position $P(i)$, x-axis along the vector $T(i+1)$. The points $T(i+1)$ and $P(i+1)$ are in $\mathbb{IF}$ required to transform in $\mathbb{EF}$ as $nT(i+1)$ and $nP(i+1)$ as given below.

$$nP(i+1) = R\left(\theta_1(i)\right) \ . \ \left[P(i+1) - P(i)\right] \tag{6}$$

$$nT(i+1) = R\left(\theta_1(i)\right) \ . \ \left[T(i+1) - P(i)\right] \tag{7}$$

$$\theta_1(i) = \arctan\left(\frac{y_{T(i+1)} - y_{P(i)}}{x_{T(i+1)} - x_{P(i)}}\right) \tag{8}$$

$$\theta_2(i) = \arctan\left(\frac{y_{P(i+1)} - y_{P(i)}}{x_{P(i+1)} - x_{P(i)}}\right) \tag{9}$$

Where, R is rotational matrix, θ_1 is angle between the $X_{inertial}$ and vector from $P(i)$ to $T(i+1)$, and θ_2 is angle between the $X_{inertial}$ and vector from $P(i)$ to $P(i+1$. The error components e_x, e_y and e_θ in $\mathbb{EF}$ is obtained as follows.

$$[e(i)]_{2\times 1} = [nP(i+1) - nT(i+1)] \tag{10}$$

$$e_x(i) = [-1\ 0] \ . \ e(i) \tag{11}$$

$$e_y(i) = [0\ 1] \ . \ e(i) \tag{12}$$

$$e_\theta(i) = \theta_2(i) - \theta_1(i) \tag{13}$$

To develop the new error functions based on the kinematics relationship of the differential robot. The component e_x responsible for translation motion, and e_y and e_θ responsible for translation motion in $\mathbb{RF}$. This can be framed in the individual error function for the right and left wheels as follows.

$$e_{\omega_L}(i) = e_x(i) + K_t \ . \ (e_y(i) + e_\theta(i)) \tag{14}$$

$$e_{\omega_R}(i) = e_x(i) - K_t \ . \ (e_y(i) + e_\theta(i)) \tag{15}$$

The above error functions e_{ω_L} and e_{ω_R} allowed the unified dual-wheel PID (UDW-PID) formulation for the ω_R, ω_L angular velocity control for respective right and left wheels in $\mathbb{WF}$. The UDW-PID considered K_t as 0.04 derived from the kinematics relationship of the differential drive robot. Additionally, aUDW-PID additional considered K_t in the tuning parameters (K_p, K_i, K_d, K_t).

IV. Results

A differential drive robot's trajectory tracking has been demonstrated using a proposed PID controller. The UDW-PID controller intuitively considered the distinct error function for the left and right wheel control. The differential drive mobile robot model parameters considered are the radius of the wheel (R = 2 cm) and the length between wheels (L = 10 cm). The three paths were taken - straight, circular, and sinusoidal. The straight reference path refers to a constant heading, the circular path represents the uniform rate of change of heading, and the sine wave path represents the variable rate of change of heading. Table I shows the PID controller behaviour considerations for trajectory tracking. The heuristic method tunes the PID controller's gains. The error functions for the left wheel given in (14) and for the right wheel is given in (15).

TABLE I: Proposed PID Controller consideration

Controller Scenario	Considerations
Case A : UDW-PID	with fixed gain $K_t = 0.04$ and tuning parameters (K_p, K_i, K_d)
Case B : aUDW-PID	with adjustable gain K_t and tuning parameters (K_p, K_i, K_d, K_t)

The mean error ME_{path} from the reference trajectory has been considered the performance index in determining the obtained path's quality, shown below.

$$\begin{aligned} ME_{path} &= \frac{1}{N}\sum_{i=1}^{N} e_D(i) \\ &= \frac{1}{N}\sum_{i=1}^{N} \left((x_{T(i)} - x_{P(i)})^2 + (y_{T(i)} - y_{P(i)})^2\right)^{\frac{1}{2}} \end{aligned} \tag{16}$$

The simulation steps N considered for each path were 100 steps. The sampling time $\triangle t$ of 0.1 seconds was considered for simulation.

A. Case A : UDW-PID controller with fixed gain K_t

The simulation result for the UDW-PID controller for the chosen reference paths. The simulation includes the actual path followed after application of UDW-PID for the right wheel angular velocity ω_R and left wheel angular velocity ω_L. The UDW-PID controller uses the same gain (K_p, K_i, K_d) to control the left and right wheels. The error function considered was distinct for each wheel.

The path obtained by UDW-PID controller for the straight line as reference trajectory is shown in Fig:3. The controller initially requires more samples to converge towards the reference trajectory as the initial position is far away from the current way-point on reference trajectory, which is also visible in the error plot with sampling instances. This resulted in aggressive action generation and can be seen as peak initially for the ω_L and ω_R control action generation.

A similar response can be observed for the circular reference trajectory shown in Fig:4. The way points are relatively far in comparison to the circular path. The jittering in the control action can be noticed, which is responsible for the circular motion due to discrete control implementation.

The path obtained for the sine wave reference trajectory is shown in Fig:5. The slight initial oscillations were observed before finally converging to the path. The aggressive control action was required to minimise the error from the reference trajectory. Due to the path's slope variation, slopes can be seen in the steady-state response.

B. Case B : aUDW-PID controller with adjustable gain K_t

In aUDW-PID control implantation for respective reference path. The K_t gain was also tuned along with convention gains (K_p, K_i, K_d) of PID controller.

The straight trajectory tracking for aUDW-PID controller is shown in Fig:3. The smoother convergence of the robot

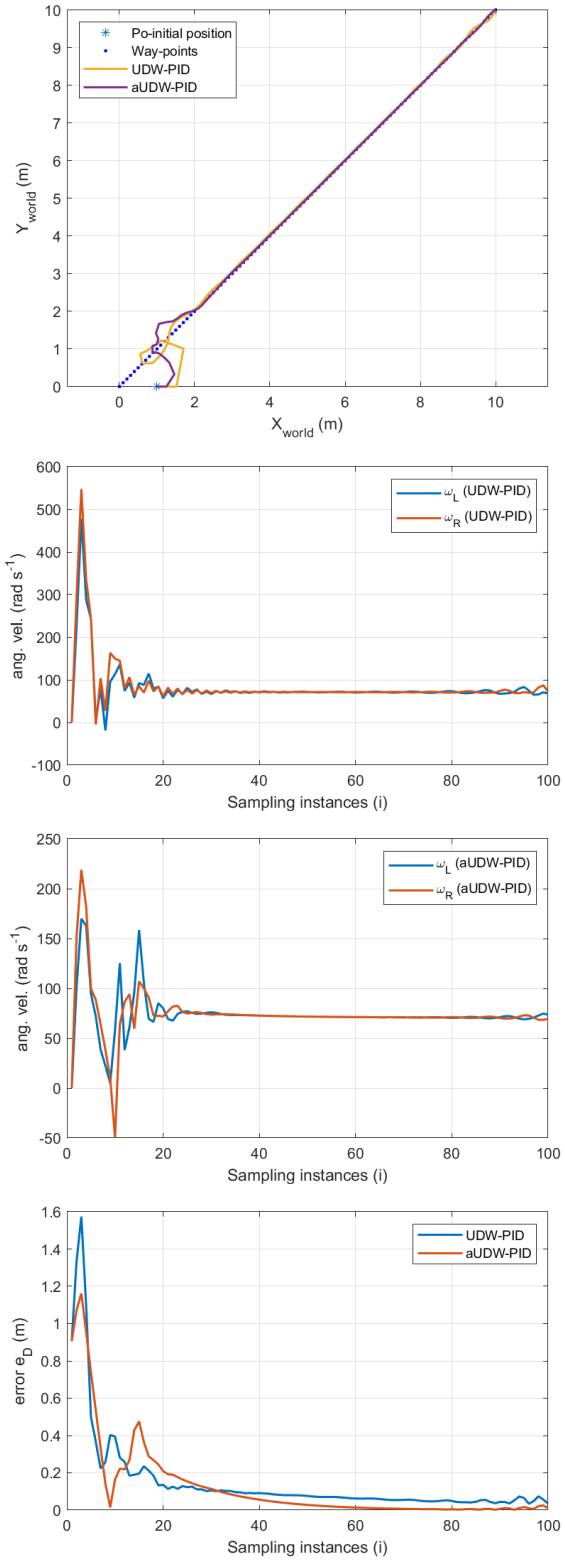


Fig. 3: Straight line trajectory tracking by proposed UDW-PID controller for fixed K_t and adaptive K_t. The control action obtained for the left wheel ω_L and right wheel ω_R is shown for both UDW-PID and aUDW-PID controller. The error from the way-point at each instance is shown for both controllers.

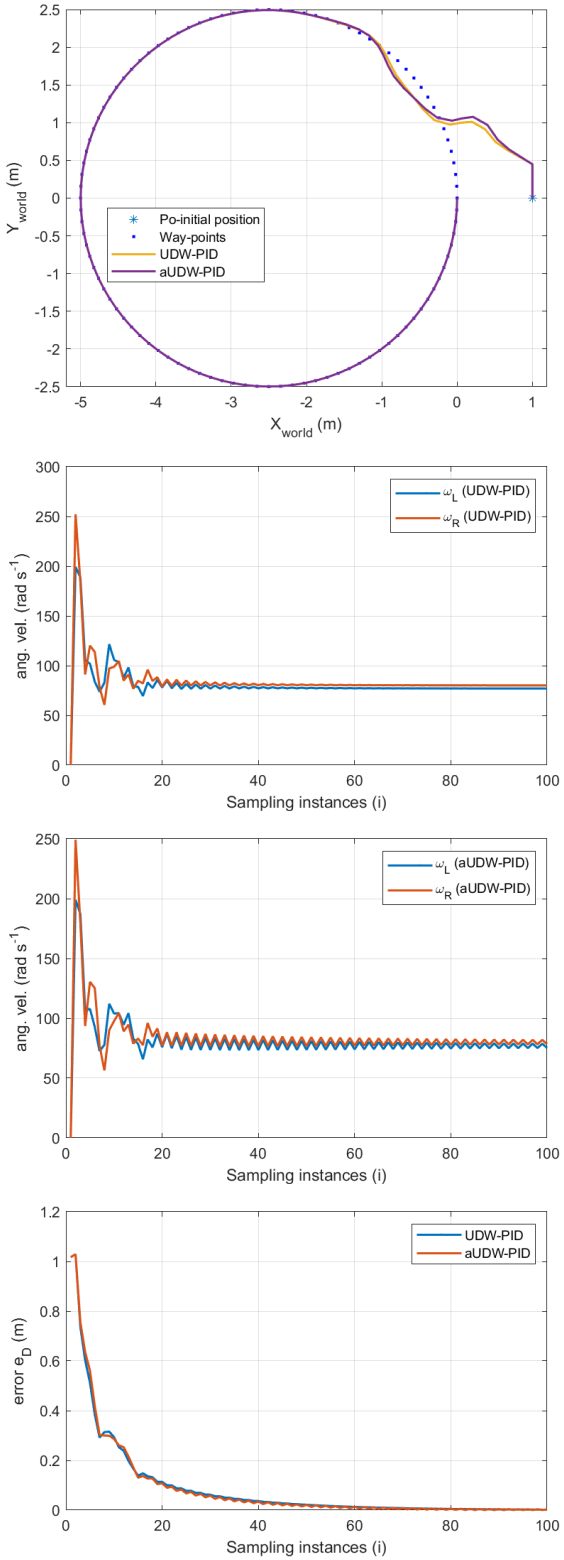


Fig. 4: Circular trajectory tracking by proposed UDW-PID controller for fixed K_t and adaptive K_t. The control action obtained for the left wheel ω_L and right wheel ω_R is shown for both UDW-PID and aUDW-PID controller. The error from the way-point at each instance is shown for both controllers.

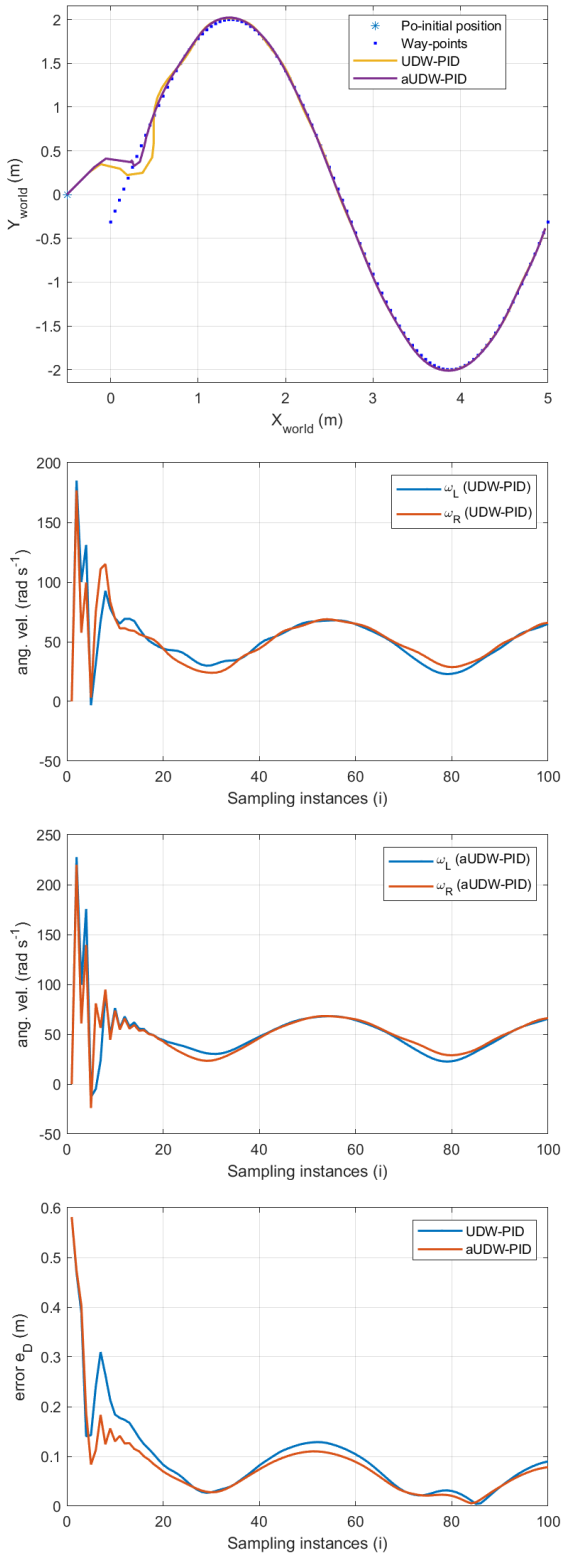


Fig. 5: Sine wave trajectory tracking by proposed UDW-PID controller for fixed K_t and adaptive K_t. The control action obtained for the left wheel ω_L and right wheel ω_R is shown for both UDW-PID and aUDW-PID controller. The error from the way-point at each instance is shown for both controllers.

trajectory towards the reference path can be observed when compared to UDW-PID controller. Due to quicker convergence of the aUDW-PID controller, more aggressive control action in ω_L and ω_R, and a swifter decline in error e_D can be observed.

A similar trajectory tracking response can be observed for the circular reference trajectory as shown in Fig:4. The control action had a slightly higher peak value and was jittering in a steady state. Overall, the error e_D was on the lower side when compared with UDW-PID.

The path obtained for the sine wave reference trajectory is shown in Fig:5, which reflects quicker convergence to the way-points. The control action during transient behaviour has a more elevated peak, resulting in a quicker drop in error e_D. For a steady state, slightly better control was achieved, resulting in considerably lower error e_D.

The overall comparison of controllers for the respective reference path is shown in Table II. The aUDW-PID yield overall lower ME_{path} due to a more aggressive control action peak, resulting in a smaller peak value in e_D. The gains obtained after the tuning using heuristic methods are also shown in Table II. The gains of aUDW-PID were on the lower side for the straight and circular path, and higher for the sine path. The gain K_t obtained for each path was found distinct, which may contribute to the overall reduction in mean path error ME_{path}.

V. Conclusions

The implementation of the PID controller for the multi-control input is a daunting task. This paper presents a unified PID control strategy for the angular velocity control of the right and left wheels of the differential drive robot. The distinction of UDW-PID control over the convectional PID control is to use a distinct error function for each wheel control, developed based on the kinematics relationship between the wheel frame and the robot frame. The unified PID control requires tuning only one set of controller gains instead of the two distinct classical PIDs needed for the right and left wheels. The UDW-PID has made the PID control implementation easier by tracking the way points of the desired reference trajectory. The simulation results for the UDW-PID controller have been demonstrated for the straight, circular and sine path, yielding smoother and quicker convergence towards the reference path and stable steady behaviour. The aUDW-PID with adaptive gain adjustment for K_t resulted in slightly better ME_{path} due to the flexibility added for selecting the respective path.

References

[1] O. Varlamov, ""brains" for robots: Application of the mivar expert systems for implementation of autonomous intelligent robots," *Big Data Research*, vol. 25, p. 100241, 2021.

[2] A. J. Critchlow, "Introduction to robotics," 1985.

[3] H. Unger, T. Markert, and E. Müller, "Evaluation of use cases of autonomous mobile robots in factory environments," *Procedia Manufacturing*, vol. 17, pp. 254–261, 2018.

[4] D. BL, "A discussion of safety issues of medical robots," *Computer integrated surgery*, pp. 287–296, 1995.

TABLE II: Mean Error path ME_{path} and PID gains obtained for several path considered for the controller

Path	**Controller**	$ME_{path}(m)$	**UDW-PID Gains**			
			K_p	K_i	K_d	K_t
Straight line	UDW-PID	0.1474	281.319	46.078	30.643	0.040
	aUDW-PID	0.1220	133.337	60.435	24.309	0.059
Circular	UDW-PID	0.0904	212.959	89.263	35.662	0.040
	aUDW-PID	0.0887	211.130	91.509	38.558	0.038
Sine Wave	UDW-PID	0.0939	306.682	44.894	19.741	0.040
	aUDW-PID	0.0802	379.887	50.530	17.907	0.030

[5] V. Venkataramanan, A. Modi, and K. Mistry, "Ai and robots impact on space exploration," *Advances in Astronautics Science and Technology*, pp. 1–9, 2024.

[6] A. V. Le, P.-C. Ku, T. Than Tun, N. Huu Khanh Nhan, Y. Shi, and R. E. Mohan, "Realization energy optimization of complete path planning in differential drive based self-reconfigurable floor cleaning robot," *Energies*, vol. 12, no. 6, p. 1136, 2019.

[7] J. Trevelyan, W. R. Hamel, and S.-C. Kang, "Robotics in hazardous applications," *Springer handbook of robotics*, pp. 1521–1548, 2016.

[8] M. A. Johnson and M. H. Moradi, *PID control*. Springer, 2005.

[9] I. Lopez-Sanchez and J. Moreno-Valenzuela, "Pid control of quadrotor uavs: A survey," *Annual Reviews in Control*, vol. 56, p. 100900, 2023.

[10] Q.-G. Wang and Z.-Y. Nie, "Pid control for mimo processes," in *PID control in the third millennium: Lessons learned and new approaches*. Springer, 2012, pp. 177–204.

[11] V. Mudeng, B. Hassanah, Y. T. K. Priyanto, and O. Saputra, "Design and simulation of two-wheeled balancing mobile robot with pid controller," *International Journal of Sustainable Transportation Technology*, vol. 3, no. 1, pp. 12–19, 2020.

[12] M. Rosenfelder, H. Ebel, J. Krauspenhaar, and P. Eberhard, "Model predictive control of non-holonomic systems: Beyond differential-drive vehicles," *Automatica*, vol. 152, p. 110972, 2023.

[13] C. Van Dang, H. Ahn, J.-W. Kim, and S. C. Lee, "Collision-free navigation in human-following task using a cognitive robotic system on differential drive vehicles," *IEEE Transactions on Cognitive and Developmental Systems*, vol. 15, no. 1, pp. 78–87, 2022.

[14] Y. Chung, C. Park, and F. Harashima, "A position control differential drive wheeled mobile robot," *IEEE Transactions on Industrial Electronics*, vol. 48, no. 4, pp. 853–863, 2001.

[15] Z. A. Leman, I. Thamrin, N. P. E. Utami, S. A. Permana, and M. B. Pamungkas, "Mobile robots with differential drive with pd pose control utilizing kinematics model," in *AIP Conference Proceedings*, vol. 2991, no. 1. AIP Publishing, 2024.

[16] M. Siwek, J. Panasiuk, L. Baranowski, W. Kaczmarek, P. Prusaczyk, and S. Borys, "Identification of differential drive robot dynamic model parameters," *Materials*, vol. 16, no. 2, p. 683, 2023.

[17] B. D. Hirpo and W. Zhongmin, "Design and control for differential drive mobile robot," *International Journal of Engineering Research & Technology (IJERT)*, vol. 6, no. 10, pp. 327–329, 2017.

[18] E. Maulana, M. A. Muslim, and A. Zainuri, "Inverse kinematics of a two-wheeled differential drive an autonomous mobile robot," in *2014 Electrical Power, Electronics, Communicatons, Control and Informatics Seminar (EECCIS)*. IEEE, 2014, pp. 93–98.

[19] G. Isoyan, "Differential drive vehicle path following and trajectory tracking with geometric control," 2024.

[20] G. Monsalve, N. B. Ltaief, V. Amoriya, and A. Cardenas, "Kinematic navigation control of differential drive agricultural robot," in *2022 IEEE International Conference on Electrical Sciences and Technologies in Maghreb (CISTEM)*, vol. 4. IEEE, 2022, pp. 1–6.